JOURNAL OF MATERIALS SCIENCE 32 (1997) 3851–3856

Delamination study using four-point bending of bilayers

J. ZHANG
TRW Space & Electronics, R6/R343, One Space Park, Redondo Beach, CA 90503 USA

J. J. LEWANDOWSKI
Department of Materials Science and Engineering, Case Western Reserve University, Cleveland, OH 44106, USA

Lamination has been shown to improve the fracture critical properties of both monolithic materials and composites. Interface delamination relaxes the stress concentration and spreads the deformation, which delays catastrophic failure and increases the Charpy impact energy. The tensile and impact properties of laminated composites depend on the interfacial strength. Bilayer laminates consisting of aluminium and aluminium composites were loaded in four-point bending. The bend bars were notched close to, but not onto, the interface. A ligament underneath the notch ranging from 0.1 mm to 0.5 mm to the interface was deliberately left in all the bend bars tested. The reasoning is that laminates can have defects or develop matrix cracks in real life situations at any location in the matrix, not necessarily at a place touching the interface. The laminates were bonded by different processes. One epoxy bonded and two types of diffusion bonded interfaces were tested. Two types of delamination have been identified: delamination without any extension of the primary crack and delamination after the extension of the primary crack into the interface. A commonly used model was employed to analyse the second mode of delamination, while a new model is proposed to predict the first type of delamination.

1. Introduction and literature

Laminated structures [1–3] have been shown to improve the fracture critical properties of both monolithic materials and composites. When laminated composites are loaded, delamination along the interface is often observed and has been identified as a mechanism for crack blunting and the spreading of deformation. The interfacial properties have been shown to greatly affect the mechanical behaviour of laminated structures [4, 5]. For example, the issue of adhesion strength has been investigated by researchers from areas as diverse as electronic packaging to composites engineering. Thus, the delamination process and the mechanics of this process are fundamental to the study of laminates.

The laminate approach has been identified as a promising technique to improve the toughness of particulate-reinforced aluminium composite materials. The level of improvement depends on the test orientation: the crack arrester direction where the primary crack is perpendicular to the interface and the crack divider direction where the crack is parallel to the interface. This paper deals only with the crack arrester direction (Fig. 1).

Four-point bending tests [6] and double cantilever beams [7] have been proposed to measure the interfacial toughness. Indentation models [8, 9] have also been developed for relating fracture toughness to indentation strength for brittle materials. Zhang and Lewandowski [10] have further extended the model to evaluate interfacial strength via indentation. In the model, the interfacial toughness is related to the delamination length and the indentation load. In studying the interface effect, most researchers choose to make the tip of the primary crack touch the interface or let the primary crack lie on the interface. In this paper, we examine the characteristics of delamination in the vicinity of a primary crack. This might be closer to the engineering situation where an undamaged laminate develops matrix cracks first when loaded. These matrix cracks can lie anywhere in the layers, not necessarily at a location reaching the interface. This paper followed up the work of Cook and Gordon [11]. They investigated the possible interfacial responses ahead of the primary crack and checked with numerical results from the finite element method. They identified three possible modes: (a) fracture of the plane of weakness ahead of the main crack; (b) fracture of interface under shear of the plane of interface symmetric about the axis of the main crack; (c) penetration of the primary crack through the interface which may or may not break afterwards. They went on to conclude that case (a) is the most probable mechanism to stop crack propagation.

In our four-point bending study, two types of delamination have been identified: delamination

0022–2461

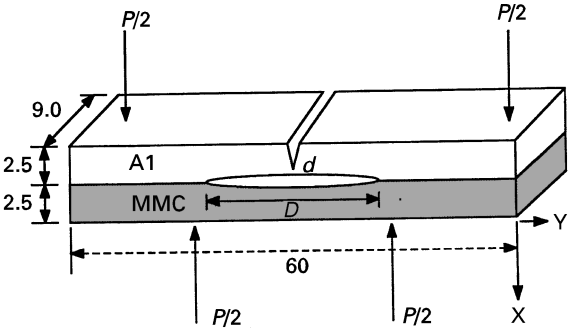

Figure 1 Four-point bend test specimens. All dimensions are in mm. The distance between two inner loading points is 2.54 cm while that between the two outer loading points is 5.08 cm.

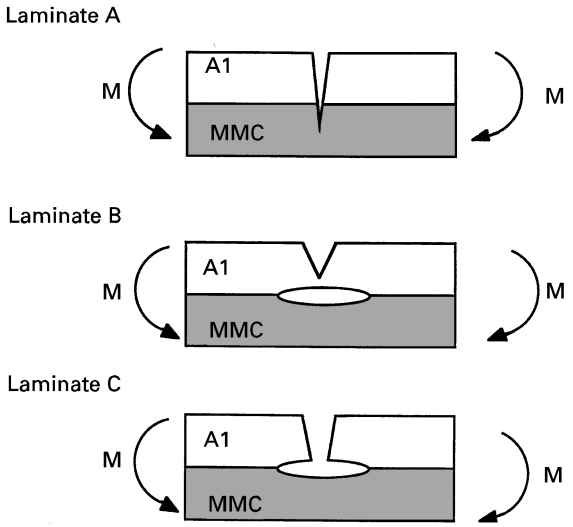

Figure 2 Three distinctive interface responses in front of an intruding crack, as typified by laminates A, B and C. (a) The primary crack ignores the interface and extends to the next layer. (b) Interface delaminates before the primary crack extends. (c) The primary crack extends first and hits the interface; then the interface starts to delaminate.

ahead of the extension of the primary crack (similar to type a of [11]) and delamination after the extension of the primary, as shown schematically in Fig. 2. Both types of delamination stop the catastrophic propagation of the primary crack. Penetration of the crack across the interface without any delamination left in the wake of the crack (similar to type c of [11]) has also been found for laminates with the strongest interfacial strength.

2. Materials and methods

Monolithic 7093 aluminium alloy and 7093 with 15% SiC reinforcement were produced in billet form through a powder metallurgy route. The billets were extruded and hot rolled to form the starting plates for the metal/composite laminates. Three types of laminates were made in collaboration with Alcoa. Laminate A was roll bonded. Laminate B was roll bonded with a 25 μm commercial purity aluminium interlayer between the aluminium layer and the composite layer. Laminate C was epoxy bonded. An overaged heat treatment in which the composite material (7093 with 15% SiC) exhibits little crack growth resistance [12] was chosen for all laminates A, B and C. This heat treatment consisted of a solution treatment of two hours at 510 °C followed by a cold water quench. The samples were then artificially aged for 24 h at 120 °C and then for 36 h at 170 °C. A separate indentation study by Zhang and Lewandowski [10] has shown that the order of the interfacial strength of laminates A, B and C is A > C > B. In the indentation study, the interfacial strength of A was found to be much higher than those of B and C, while C has a slightly higher bond strength than B.

Bend bars with 60 mm in length, 5 mm in thickness and 9 mm in width were subsequently machined (Fig. 1). All the specimens were polished using fine grade SiC papers to at least a 3 μm finish. A 12.5 cm diamond saw was used to notch the bilayer specimens perpendicular to the interface. The notch has a distance ranging from 100 to 500 μm to the interface.

Four-point bending testing was conducted on the specimens using an Instron 1125 universal machine under displacement control with a crosshead speed of 0.5 mm min^{-1}. The slow speed was chosen since the crack extension and delamination could be observed better. The laminates were tested in such a way that the notched layer was loaded in tension. A travelling microscopy together with a t.v. monitor was used to record the deformation and failure process.

3. Results

Slow four-point bend tests were performed on all three types of laminates. Three distinctive types of interface responses were observed. In laminate A, the primary crack ignores the interfaces and runs into the bottom layer (shown schematically in Fig. 2a). In laminate B, the interface delaminates before the primary crack extends (Fig. 2b). In the case of laminates C, the primary crack first extends to the interface and then delamination follows (Fig. 2c). Figs 3–5 show the optical microscopy view of the laminates A, B and C after primary crack extension. Figs 6–8 show the load–displacement curves of the laminates A, B and C. In the case of laminates A and C, the peak corresponds to the load right before the extension of the primary crack while the peak load corresponds to the load before the delamination of the interface in the case of laminate B. The delamination moment of laminate B and C is taken as the load at the dip right after the peak (Figs 4 and 5). Eight specimens were tested on laminates A, B and C. The specimen geometry and delamination moment are tabulated in Table I.

Two specimens of laminates A were tested. When the specimens were examined under an optical microscope, the interface was found to be intact (Fig. 3). No interface delamination was observed. Essentially, the primary crack extended from the aluminium layer into the composite layer as if the interface was not there. As a result, no toughening from delamination is achieved and the crack propagates rather freely across the interface. However, the toughness of the laminate exceeds

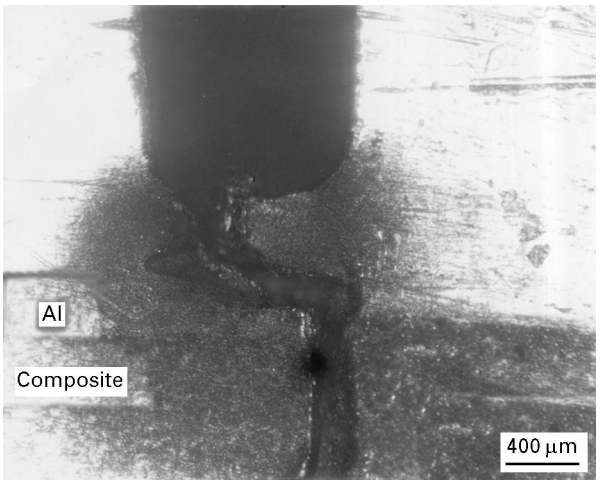

Figure 3 Optical micrograph showing the extension of the primary crack into the composite layer in laminate A.

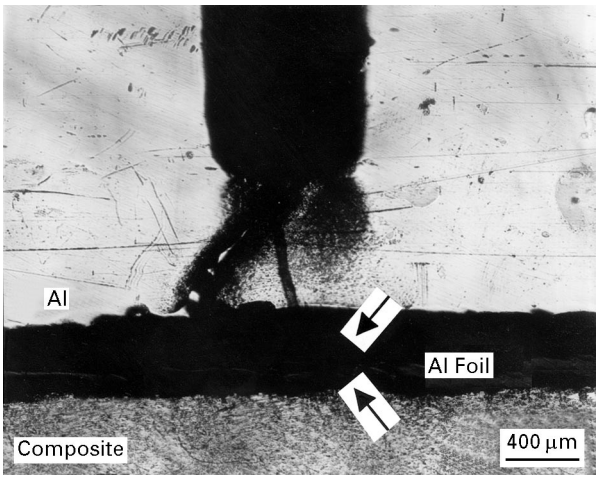

Figure 4 Optical micrograph showing the delamination in the interface and the extension of the primary crack into the interface in laminate B. It is worth noting that the delamination occurred on both sides of the pure aluminium interlayer, indicated by the arrows. The crack extension occurred afterwards, corresponding to the second load drop in the load–displacement curve.

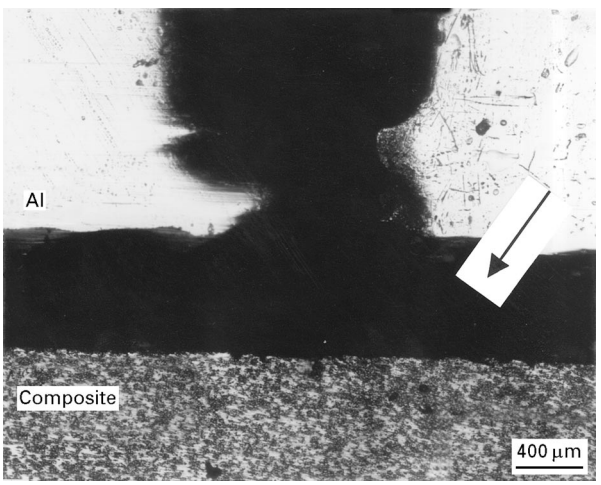

Figure 5 Optical micrograph showing the delamination in the interface and the extension of the primary crack into the interface in laminate C. It should be noted that crack extension is followed almost immediately by the delamination. The arrow indicates delamination.

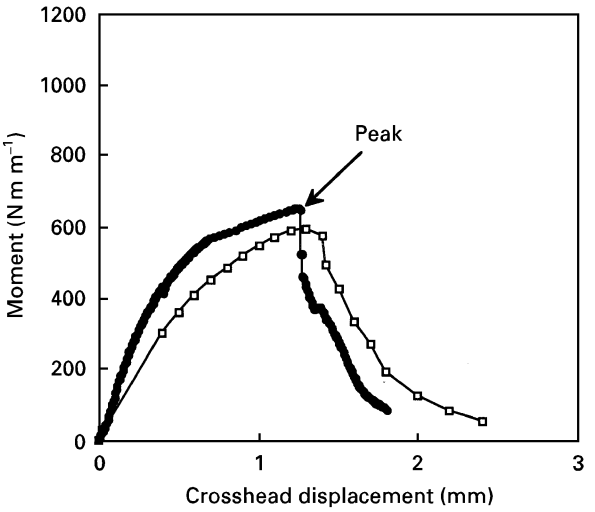

Figure 6 The moment–displacement curves of laminate A. Significant plastic deformation with visible necking was found on the back and front surfaces of the beam in the region between the notch and the interface, corresponding to the non-linear part of load–displacement curve before the peak load. (□) A1 (d = 0.24 mm); (●) A2 (d = 0.48 mm).

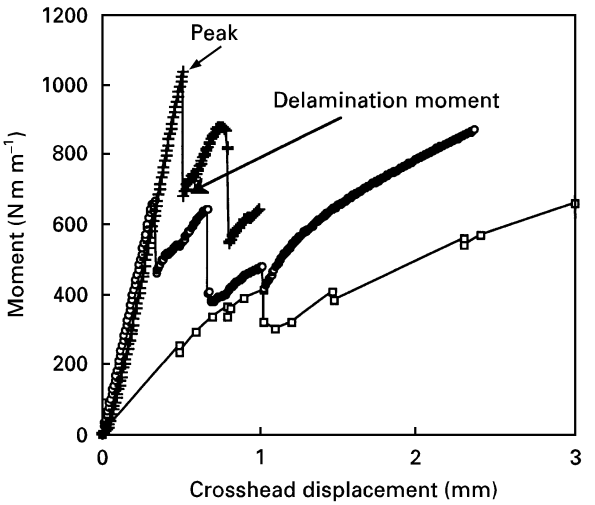

Figure 7 The moment–displacement curves of laminate B. The delamination moment is taken as the moment at the dip after the first peak moment. (□) B1 (d = 0.13 mm); (○) B2 (d = 0.32 mm); (+) B3 (d = 0.53 mm).

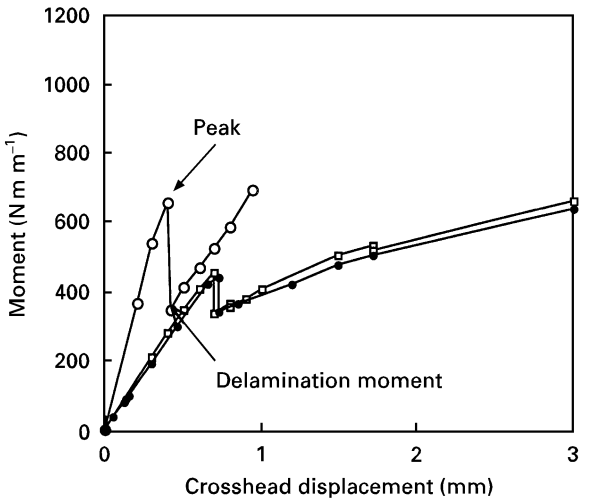

Figure 8 The moment–displacement curves of laminate C. The delamination moment is taken as the moment at the dip after the peak moment. (●) C1 (d = 0.2 mm); (□) C2 (d = 0.24 mm); (○) C3 (d = 0.45 mm).

TABLE I Test results of bilayer laminates

Specimen	d (mm)	Peak moment (N m m^{-1})	Delamination moment (N m m^{-1})	Interface, G_i (J m^{-2})	Interface K_i (MPa m$^{0.5}$)
A1	0.24	665	–	–	–
A2	0.48	601	–	–	–
B1	0.13	410	300	–	–
B2	0.32	663	467	–	–
B3	0.53	1035	680	–	–
C1	0.2	440	340	432	5.50
C2	0.24	455	339	429	5.48
C3	0.45	660	346	447	5.59

that of the 100% composite beam, as shown elsewhere [2, 13]. The laminate [2] exhibited an increase in bend ductility over the 100% composite beam in quasi-static bending tests. The laminate [13] also demonstrated a higher impact energy absorption and a higher capacity of deflection than the 100% composite beam in pendulum impact testing.

For laminates B, delaminations occurred before the extension of the primary crack from the notch in all three specimens. The closer the initial primary crack to the interface, the higher the moment at delamination (Fig. 7). The behaviour of the interface at the centre of the beam was monitored by an optical microscope attached to a video recorder and a t.v. screen. It was found that the delamination extended at a high speed for at least 15 mm along the interface before it was arrested. Upon further load increase, the delamination started to grow steadily. It should be noted that the peak load corresponds to the onset of the initial high speed delamination while the moment at the first dip (defined as the delamination moment) is the load for stable state delamination.

Delamination in the case of laminate C is different again. The primary crack first propagate to the interface, followed by immediate delamination. The bending moment delamination is almost constant in the range of d tested (Fig. 8). One can argue that the distance of the initial crack to the interface does not matter since the delamination occurs after the crack reaches the interface. The moment at delamination then represents the amount of force needed to drive the crack along the interface further, which depends on the interfacial strength and the available energy stored in the upper and lower beams. Once the primary crack hits the interface and starts to deflect along the interface, the crack geometry is identical to the four-point bending of bilayer beams investigated by Charalambides *et al.* [6]. According to these researchers, the strain energy release rate should exhibit steady-state characteristics at least when the interfacial crack exceeds the thickness of the upper layer of the beam. The steady-state value, G_{SS}, is the difference in the strain energy in the uncracked and cracked beam. They gave the following

$$G_{SS} = \frac{M^2(1-\nu_2^2)}{2E_2}\left(\frac{1}{I_2} - \frac{\lambda}{I_c}\right) \quad (1)$$

where $\lambda = E_2(1-\nu_1^2)/E_1(1-\nu_2^2)$; the subscripts 1 and 2 refer to the top notched layer and the lower layer and the subscript c refers to the composite beam; E and ν are Young's modulus and Poisson's ratio. M and I are the applied moment and moment of inertia per unit width. With P being the total applied load, b the beam width and l the spacing between the inner and outer loading lines, we have

$$M = Pl/2b \qquad \text{and } I_2 = h_2^{3/12} \quad (2)$$

where h_2 is the thickness of the lower layer. Using the materials constants $E_2 \approx E_1 = 72$ GPa; $\nu_1 = \nu_2 = 0.3$, the dimensions of our specimens and the delamination moment from our experiments, the critical energy release rate of the interface can be calculated (Table I).

The average value of critical energy release rate for the interface of laminate C is around 400 J m^{-2}. This is close to the estimate of critical energy release rate for epoxy [14]. For the second mode of delamination, Charalambides' model [6] seems to be able to predict the interface growth toughness or the delamination moment if the growth toughness is known. It should be noted that the model is not suitable for the analysis of delamination in laminate B since the delamination process is totally different. Also, the model is not suitable for predicting the peak moment or the moment at the onset of delamination.

For laminates A, B and C, the peak load increases with increasing d. This is expected. Laminates are stronger when the main matrix cracks or the defects are smaller. From the load–displacement trace, the peak load occurred in the linear elastic range for laminate B and C, indicating that small scale rather than widespread yielding dominates before the peak load. For laminate A, significant plastic deformation with visible necking was found on the back and front surfaces of the beam in the region between the notch and the interface, resulting in a non-linear relationship of load–displacement in Fig. 6.

4. Discussion and conclusions

The defects and the matrix cracks in laminated structures under static loading or impact may occur in many locations at a distance to the interfaces. In comparison to the three scenarios envisioned by Cook

and Gordon [11], our experimental results demonstrated three possibilities of the crack–interface interaction depending on the magnitude of the interfacial strength:

1. When the interfacial strength is high, the crack will penetrate through the interface, like the case of laminate A. No major benefit from delamination will materialise in this case. However, the laminate still exhibits higher toughness than a 100% composite beam, as shown elsewhere [2, 13].
2. If the interfacial strength is weak, the delamination will occur ahead of the main crack, like the case of laminate B.
3. If the bond strength is intermediate, the crack will be deflected along the interface after it extends and hits the interface, like the case of laminate C. The catastrophic propagation of the primary crack is retarded.

The stress concentration is relaxed and the deformation is spread more in the first type of delamination (i.e. laminate B) than the second type (i.e. laminate C). It seems that the benefit of built-in interfaces is maximized in the first type (i.e. laminate B) among all the three types of interface responses typified in laminates A, B and C. This is not to say the best laminates will be made with the weakest interface. It is clear that the purpose of stopping the crack propagation could be achieved if no adhesion at all exists in the interface. On the other hand, the laminates would have no strength when loaded in tension normal to the interface. Interlaminar strength and structural integrity are always concerns in design.

We are aware that some local yielding occurs when this type of laminated aluminium composites are loaded. However, the peak load was found to occur in the linear elastic range of global force–displacement curve for laminate B and C. A linear fracture mechanics model is developed here to model their damage process.

Since the bending rigidity of the aluminium composite layer with 15% SiC reinforcement is not very different from the aluminium layer, we ignore the difference in our stress calculation below. The bonding between layers is assumed to be perfect before delamination occurs. The stress intensity factor for four-point bending can be calculated as follows [15]

$$K_{\mathrm{I}} = \frac{3Pl}{bh^2}(\pi a)^{0.5} f(a/h) \tag{3}$$

where $f(a/h)$ is a geometrical factor and h is the thickness of the beam

$$f(a/h) = 1.122 - 1.121(a/h) + 3.74(a/h)^2 + 3.873(a/h)^3 - 19.05(a/h)^4 + 22.55(a/h)^5 \tag{4}$$

$$(\sigma_x, \sigma_y, \tau_{xy})$$

The stresses at the interface right below the primary crack (Fig. 1) are

$$\sigma_x = \frac{K_{\mathrm{I}}}{(2\pi d)^{0.5}} \tag{5}$$

$$\sigma_y = \sigma_x \tag{6}$$

$$\tau_{xy} = 0 \tag{7}$$

The interface is assumed to start delamination when the maximum tensile stress across it reaches the interfacial strength. This leads to

$$\frac{K_{\mathrm{I}}}{(2\pi d)^{0.5}} = \sigma_{\mathrm{f}} \tag{8}$$

where σ_{f} is the strength of the interface. Then, we have

$$\frac{3Pl}{bh^2} f(a/h) = \sigma_{\mathrm{f}} (2d/a)^{0.5} \tag{9}$$

where $a = h/2 - d$ (see Fig. 1).

The peak moment in the load–displacement curve for laminate B correlates with the initiation of delamination. The following relationship can be established between the distance d and the peak moment M_{P}

$$M_{\mathrm{P}} = 0.235\, \sigma_{\mathrm{f}} \frac{h^2}{(0.5h - d)^{0.5}} \frac{d^{0.5}}{f(0.5 - d/h)} \tag{10}$$

This type of functionality indeed seems to agree with the experimental data for the peak moment for laminate B (Fig. 9). The fitting of experimental data for laminate B gives the following value for the interfacial strength of laminate B: $\sigma_{\mathrm{f}} = 400$ MPa. It is worth noting that the delamination moment for laminate B also seems to follow a linear relation with d in the range of distance tested (Fig. 9).

The peak moment in the load–displacement curve for laminate C correlates with the extension of the primary crack from the notch. By equating the stress intensity factor in Equation 3 to the fracture toughness K_{IC} of the aluminium matrix, the peak moment for laminate C can be calculated as follows

$$M_{\mathrm{P}} = K_{\mathrm{IC}} \frac{h^2}{6[\pi(0.5h - d)]^{0.5} f(0.5 - d/h)} \tag{11}$$

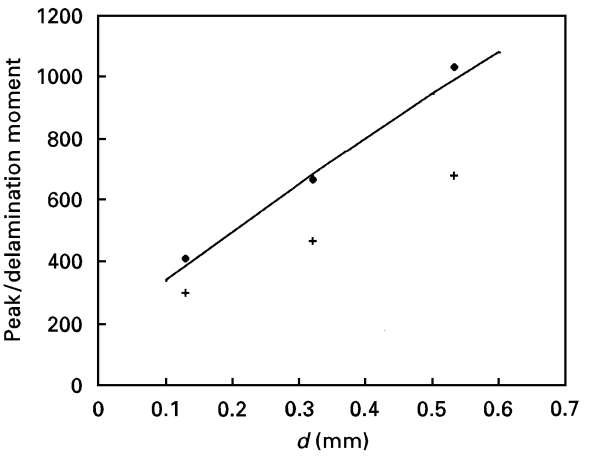

Figure 9 The peak (◆) and delamination (+) moments against the distance d for laminate B. The dotted line indicates prediction by Equation 10 of the peak moment.

Equation 11 has a weak dependence on d than Equation 10. Indeed the peak moment for laminate C demonstrated a much weaker dependence than that for laminate B.

In conclusion, the interfacial strength has a great deal of influence on the pattern of damage accumulation. In general, a weak interface will promote the second type of delamination (i.e. laminate C), while a strong interface will not delaminate at all (i.e. laminate A). At intermediate strength, the first type of delamination (i.e. laminate B) dominates where the interface delaminates after the primary crack reaches the interface.

Acknowledgements

Thanks are due to Todd Osman at Case Western Reserve University for providing the laminated specimens for the tests.

References

1. Y. LENG and T. C. COURTNEY, *Metall. Trans. A* **21A** (1990) 2159.
2. L. Y. ELLIS and J. J. LEWANDOWSKI, *J. Mater. Sci. Lett.* **10** (1990) 461.
3. S. LEE, J. WADSWORTH and O. D. SHERBY, *J. Comp. Mater.* **25** (1991) 842.
4. V. C. NARDONE, J. R. STRIFE and K. M. PREWO, *Metall. Trans. A* **22A** (1991) 171.
5. W. H. HUNT, T. M. OSMAN and J. J. LEWANDOWSKI, *J. Metals*: **45** (1993) 30.
6. P. G. CHARALAMBIDES, J. LUND, A. G. EVANS and R. M. McMEEKING, *J. Appl. Mech.* **56** (1989) 77.
7. L. K. JAIN and Y. -W. MAI, *Comp. Sci. Tech.* **51** (1994) 331.
8. A. G. EVANS and E. A. CHARLES, *J. Amer. Ceram. Soc.* **59** (1976) 371.
9. G. R. ANSTIS, P. CHANTIKUL, B. R. LAWN and D. B. MARSHALL, *ibid.* **64** (1981) 533.
10. J. ZHANG and J. J. LEWANDOWSKI, *J. Mater. Sci.* **29** (1994) 4002.
11. J. COOK and J. E. GORDON, *Proc. Roy. Soc., A* **282** (1964) 508.
12. M. MANOHARAN and J. J. LEWANDOWSKI, *Acta Metall.* **38** (1990) 489.
13. L. Y. ELLIS and J. J. LEWANDOWSKI, *Mat. Sci. Eng., A* **183** (1994) 59.
14. M. F. ASHBY and D. R. H. JONES, "Engineering materials: an introduction to their properties and applications" (Pergamon Press, Oxford, 1985).
15. Y. MURAKAMI (ed.), "Stress intensity factors handbook", Vol. 1 (Pergamon Press, Oxford, 1987).

Received 7 September 1995
and accepted 15 January 1996